Frenkel pairs in low-temperature electron-irradiated InP: Optical-absorption spectroscopy

H. Hausmann and P. Ehrhart
Institut für Festkörperforschung des Forschungszentrums Jülich, D-52425 Jülich, Germany
(Received 30 September 1994; revised manuscript received 6 February 1995)

Semi-insulating InP (Fe) wafers were irradiated at 4.5 K with 2.2-MeV electrons. The irradiation dose was varied between 2×10^{17} e^-/cm^2 and 3×10^{18} e^-/cm^2 and the samples were transferred in liquid nitrogen to an optical cryostat for the investigation of the magnetic circular dichroism of the optical absorption (MCDA) and the infrared absorption. After irradiation we observed two new MCDA spectra that increase linearly with dose and are attributed to close Frenkel pairs. These spectra anneal around 200 K (stage I) and seem to represent the spectroscopic evidence for intrinsic defects that anneal below room temperature. Along with the annealing of these close Frenkel pairs, two well-known MCDA spectra appear that had been related to the P_{In} antisite and to impurity-defect complexes, respectively. The impurity-defect complexes anneal between 330 and 400 K (stage II) whereas the final annealing of the P_{In} antisites is observed around 650 K. Along with this final annealing the MCDA band of the Fe acceptor is completely recovered. A well-known infrared absorption band ($E_{photon}\geq0.77$ eV) is shown to be directly formed during irradiation. The underlying defect reactions are discussed with special emphasis on the correlation to previously published diffuse x-ray-scattering results.

I. INTRODUCTION

In a preceding paper[1] we showed by x-ray-diffraction methods that very high concentrations of intrinsic point defects can be produced in InP by low-temperature electron irradiation, and that there is a major annealing stage of these defects below room temperature. As x rays yield an average signal over the contribution of all defects independent of their charge state, the present investigation was initiated to supplement these results with some spectroscopic results on specific defects. Due to the high sensitivity of the spectroscopic methods there is also a better overlap with published data that refer mostly to low-dose irradiations. Of special interest was the search for intrinsic defects that anneal at low temperatures, as the present information from deep-level transient spectroscopy (DLTS) refers only to impurity-defect complexes as discussed in Ref. 1.

The magnetic circular dichroism of the optical absorption (MCDA) and optical-absorption spectroscopy (OAS) were used for this investigation, as these methods can be applied starting from the lowest temperatures and can be used over a rather wide range of irradiation doses. OAS—and especially MCDA—spectra can generally not be related directly to first-principles defect calculations because of the complexity of the optical transitions that involve the ground state as well as the excited states of a point defect. However, the paramagnetic MCDA can be related directly to spectra obtained by electron paramagnetic resonance (EPR) from the same paramagnetic ground state [via optically detected EPR (ODEPR) and electron nuclear double resonance (ODENDOR)]. Therefore MCDA spectra can be used as fingerprints for defects that have been identified by these techniques. There are no fingerprints available as observed directly after low-temperature irradiation; however, several very specific fingerprints have been investigated in as-grown InP and after irradiation at room temperature.

(i) The MCDA of the Fe dopand in InP has been investigated in detail,[2–4] and is attributed to the neutral and paramagnetic charge state of the Fe_{In} acceptor that is the Fe^{3+} charge state with a spin $S=\frac{5}{2}$. The MCDA is characterized by a broad band with a dominating maximum at a photon energy of 1.25 eV (see Figs. 2 and 8 below; further details of the spectra are not visible on that scale). In the following we will use the energy of the position of this maximum in order to characterize this fingerprint: the 1.25-eV MCDA band.

(ii) The P_{In} antisite is a double donor that was first observed by EPR after room-temperature (RT) irradiation of *p*-type InP.[5] In contrast to some earlier conclusions, recent investigations[6,7] consistently locate the $P_{In}^{+/2+}$ transition level within the upper half of the band gap and the $P_{In}^{0/+}$ level resonant with the conduction band. Nevertheless, the exact position may depend on the type of material and/or the defect concentration. For bulk samples the $P_{In}^{+/2+}$ transition has been estimated to be at $E_v+(1.1\pm0.1)$ eV and the $P_{In}^{0/+}$ level at $E_v+(1.39\pm0.03)$ eV,[7] whereas for molecular-beam epitaxy (MBE)-grown epilayers $P_{In}^{+/2+}$ has been located at $E_c-0.23$ eV and $P_{In}^{0/+}$ at $E_c+0.12$ eV;[6] using a low-temperature band gap of ≈1.42 eV, this yields $E_v+1.19$ and $E_v+1.54$ eV for the epilayers. The paramagnetic MCDA spectra observed for the P_{In}^{+} state have been identified by ODEPR and ODENDOR (Refs. 7–13) in irradiated as well as as-grown InP. Remarkably this defect has in some cases also been observed for *p*-type samples; these observations have been explained by a two-step excitation.[7] The MCDA spectrum is characterized by a broad band peaking between 1.3 and 1.4 eV, i.e., very close to the band edge. The exact position of the peak therefore depends on the instrumental and/or background corrections, and it has been argued that this spectrum has to be considered the tail of the band with its

center above the band-edge energy.[9] As this peak position is not well defined, detailed optically detected magnetic-resonance investigations have been performed with light energies between 1.26 (Ref. 12) and 1.36 eV.[7] We will characterize the amplitude of this MCDA band by its value at 1.32 eV, and call it for short the 1.32-eV MCDA band. At this energy the background due to other defects is in addition very low: The Fe^{3+} band has a zero crossing, and some other doping-dependent spectra are closer to the band edge.[7,12] Detailed ENDOR investigations[7] revealed at least three different P_{In} configurations that are, however, all characterized by the same EPR and very similar MCDA spectra. P_{In} in the as-grown samples was attributed to the isolated antisite, and the differences observed for irradiated InP have been tentatively attributed to disturbances by acceptors, possibly V_{In} in the second neighbor shell. The insensitivity of the MCDA to the details of the defect structure is in contrast to the observations for the As_{Ga} antisite in GaAs, where different spectra have been observed,[14] and might be due to the limited range of the spectra that are cut off within the first peak by the band edge.

(iii) An additional MCDA band with a zero crossing at 1.06 eV has been observed after RT electron irradiation in semi-insulating (s.i.) as well as in p- and n-type InP.[12,13] This MCDA anneals very similar to the $E11$ and $H4$ DLTS traps within annealing stage II ($\approx$370 K). Therefore this MCDA has been attributed to the same complex consisting of an impurity and an irradiation defect, probably P_i or V_p.[12] This MCDA spectrum is most specifically characterized by the energy of the zero crossing, and is therefore called[13] the 1.06-eV MCDA band.

(iv) In addition to the MCDA an absorption band with an onset at 0.77 eV has been observed after RT electron irradiation.[15] This band has been attributed to an ionization transition, and also anneals within stage II. The underlaying defect is produced with a rather high introduction rate ($\sum \approx n_d/\phi t \approx 1$ cm^{-1}, where n_d is the defect density, and ϕt is the total dose), and there is no saturation up to an irradiation dose of 10^{18} e^-/cm^2.[15] Unfortunately, so far there is no model for the underlying defect. As the band is most specifically characterized by the onset energy,[15] we will refer to this fingerprint as the 0.77-eV absorption band.

Starting from these fingerprints, we investigated the low-temperature defect production and the defect reactions during an isochronal annealing program. In order to compare the results with x-ray investigations, we extended the irradiations to rather high doses. The systematic investigation of a wide range of irradiation doses allows in addition a direct discrimination between intrinsic defects and possibly impurity-related defect complexes, as the latter must show a saturation behavior at quite low concentrations that correspond to the doping of 2×10^{15} Fe/cm^3. In order to facilitate these observations we started with semi-insulating InP, where only small changes of the position of the Fermi level are expected during prolonged irradiation, as independent of the doping InP becomes highly Ohmic and n type after a critical irradiation dose at RT [$\phi t(e^-/cm^2) \geq c_{dop}(cm^{-3})$].[12,6] Hence irradiated InP is considered semi-insulating,[12] although more specifically the Fermi level moves to the upper half of the band gap and is finally located at $E_c-(0.3-0.4)$ eV.[16,17] Using standard wafer thicknesses the absorption close to the band edge becomes rather high, and sets a limit to the low-temperature experiments at a dose of $\approx10^{18}e^-/cm^2$, or to defect concentrations $\approx10^{18}/cm^3$.[1]

In Sec. II we give a short introduction to the experimental techniques. In Sec. III, we present experimental evidence of the different fingerprints, and in Sec. IV we discuss conclusions on the defect reactions.

II. EXPERIMENT

A. Magnetic circular dichroism of the absorption

The MCDA is defined as the differential absorption of the sample for right (+) and left (−) circularly polarized light that propagates along the direction of the applied magnetic field (see Ref. 18 for review)

$$\epsilon=\frac{d}{4}(\alpha_- - \alpha_+) \tag{1}$$

with $\alpha\pm$ being the respective absorption coefficients and d the thickness of the sample. Within a good approximation this quantity can be experimentally determined from the intensities of the transmitted light of polarization $\pm$: $\epsilon=\text{const}\times x_{MCDA}$ with

$$x_{MCDA}=(I^+-I^-)/(I^++I^-)\ . \tag{2}$$

The constant factor is characteristic for the special experimental equipment and is essentially determined by the exact degree of polarization. As we do not discuss the absolute values of the dichroism in the following we will present the MCDA spectra as defined above.

The origin of the MCDA is schematically explained in Fig. 1 for the most simple example of the paramagnetic MCDA of a lattice defect: the defect may be characterized by an unpaired electron with $s=\frac{1}{2}$ in a doublet ground state and an excited state, which both split in the presence of the magnetic field. In addition to the fundamental transition cross sections σ_+ and σ_- the paramagnetic MCD depends on the population numbers N^+ and N^- of the Zeeman levels. Low temperatures and high fields are therefore favorable for a good sensitivity. Of course there is a saturation if $N^+\rightarrow0$, and on the other extreme there might be only a small diamagnetic MCD signal left at high temperatures where both sublevels are equally occupied. Generally MCD transitions are possible to several excited states, and the spectra are more complex. On the other hand, this complexity makes the MCDA a sensitive fingerprint for specific defects once they are identified, e.g., by EPR and/or ENDOR (e.g., Ref. 14).

MCDA spectra were generally taken at 2 K with an applied magnetic field of 5.73 T. The light from a 100-W halogen lamp passed through a $\frac{1}{4}$-m double monochromator, and was polarized by a combination of a Glan Thomson prisma and a photoelastic modulator working at 50

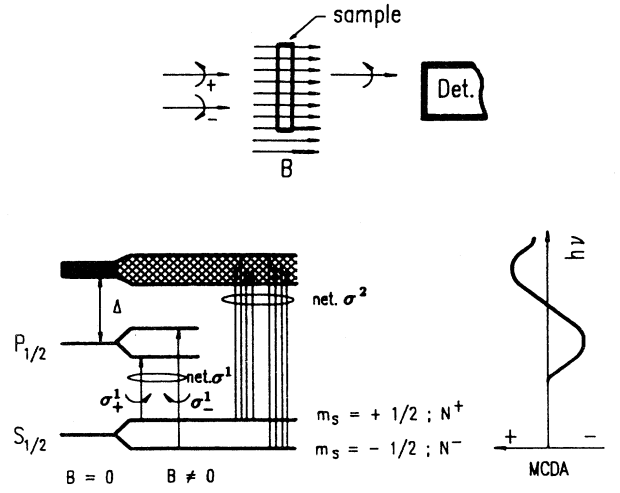

FIG. 1. (a) Schematic view of the MCDA experiment and (b) of underlying optical transitions. The optical transitions from a $S_{1/2}$ ground state to a first excited state ($P_{1/2}$) and to higher excited states that are separated by an energy gap Δ (the spin-orbit splitting) are shown. σ^1_+ and σ^1_- transitions yield a first negative MCDA peak with a net cross section σ^1, and transitions to higher excitations yield a net cross section σ_2 of the MCDA with opposite sign.

KHz. Without calibration the sign of the MCDA [Eq. (2)] may depend on a phase shift between the modulator and the detection system. Our spectra have all the same absolute signs of the MCDA amplitudes and correspond, e.g., to a positive sign of the maximum at 0.95 eV of the $EL2^+$ in GaAs. A cooled Ge detector was used for photon energies between 0.7 eV and the absorption edge (for details, see Refs. 19 and 20). For a direct comparison of the slightly different samples, all spectra were normalized to correspond to a sample thickness of 100 μm.

During measurements the sample could be illuminated via a mirror from a side entry by a second light source in order to change the population of the defect levels by optical transitions. In this way it is sometimes possible to observe defect states that are not populated in thermal equilibrium for a given position of the Fermi level. As the absolute magnitude of the effects of this optical pumping is small, we will discuss only the changes of the spectra, i.e., the difference of the spectra with and without additional illumination, and characterize these spectra by the index p ($MCDA_p$). The energy of the pumping light was selected by different band-pass filters and the intensity of this light at the position of the sample was $\simeq 15-20$ mW/cm^2. Using the same light source with a long pass filter ($\lambda \geq 850$ nm; power at the sample: ≈ 200 mW/cm^2), we tested the sensitivity of the defect spectra to optical quenching by illuminating the sample for 10 min at 2 K. This procedure quenches the EL2 defects in GaAs within seconds; however, no quenching effect was observed for the present defects in InP. This behavior is in agreement with published results as only in neutron-irradiated InP has an effect of the photoquenching been observed in InP.[21]

B. Samples and irradiations

Samples of sizes 12×6 mm^2 were cut from [100]-oriented InP (2×10^{15} Fe cm^{-3}) wafers and polished to obtain a final thickness of 330 μm. These samples were irradiated at 4.5 K with 2.2-MeV electrons in a similar way to the samples for the x-ray investigations.[1] The irradiation doses were No. 1: 0.2, No. 2: 0.35, No. 3: 0.85, and No. 4: 2.8×10^{18} e^-/cm^2. After the highest irradiation dose the optical transmission, especially close to the band edge, was too low for quantitative measurements. Therefore the sample was additionally polished to a final thickness of 120 μm. As the sample warmed up to about 80°C during this polishing, no data are available at lower temperatures for this sample.

After irradiation the samples were transferred in liquid nitrogen into the optical cryostat. The annealing of the samples was performed within an isochronal program with holding times of 15 min. Anneals at temperatures $T_a \leq$ RT were performed within the He atmosphere of the cryostat, and at higher temperatures within an external furnace under vacuum ($p \leq 10^{-4}$ Pa).

III. IDENTIFICATION OF THE FINGERPRINTS

In this section we present an observation of the different MCDA fingerprints separately, and in the same order as they are observed to appear and anneal, respectively. The optical absorption is presented in the final Sec. III D.

A. New MCDA spectra after low-temperature irradiation

After irradiation the MCDA band of the Fe acceptors is no longer visible, and a completely different spectrum is observed. Figure 2 shows that this MCDA is characterized by a peak at 1.17 eV and a negative peak at 1.27 eV of about twice that amplitude. Figure 3 shows that the sizes of both of these peaks increase linearly with the

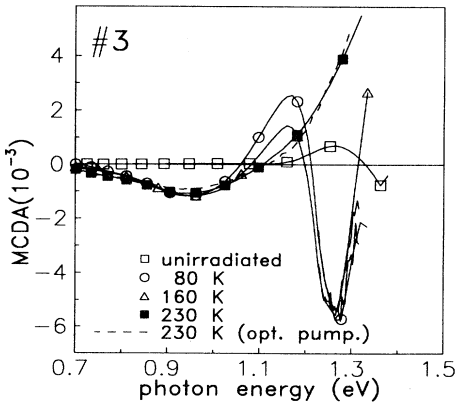

FIG. 2. Characteristic MCD spectra observed after irradiation and annealing up to RT of sample 3 ($\phi t = 8.5\times10^{17}$ e^-/cm^2). After the 230-K anneal the MCDA is shown in addition, as observed under simultaneous optical pumping with a bandpass filter BP1200. The different symbols characterize the different spectra and not the measuring points for the spectra that are not resolved in these plots.

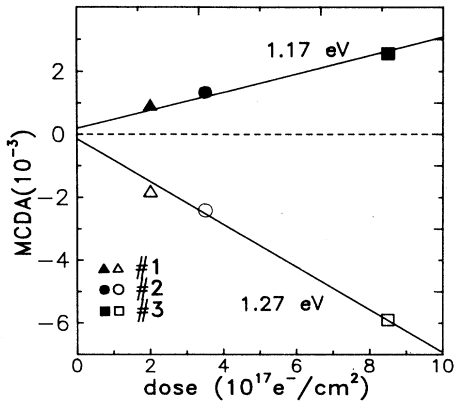

FIG. 3. Dose dependence of the amplitude of the positive and negative peaks at 1.17 and 1.27 eV, respectively, as observed after irradiation (annealing temperature $T_a = 80$ K).

irradiation doses, and this behavior is a strong indication of an intrinsic underlying defect. In spite of this common feature the annealing behavior (Figs. 2 and 4) of the two peaks is different, and the 1.17-eV peak anneals faster than the 1.27-eV peak. Hence the two peaks must originate from two different defects. As can be seen from Fig. 2 there arises another dominating spectrum (i.e., the P_{In} antisite) along with the seemingly complete annealing at 230 K such that a remaining small part of the low-temperature peaks and minor differences in their final disappearing could not be detected.

The missing visibility of the MCDA band of Fe^{3+} is in agreement with the EPR investigations of Fe acceptors in electron-irradiated InP, that showed a change of the spectrum by the trapping of defects at 77 K.[22] The resulting spectra cannot, however, be attributed to these Fe-defect complexes: First, the signal disappears at $T_a = 230$ K, whereas the number of complexes of Ref. 22 is stable up to RT and increases before the final annealing between 400 and 500 K. Second, the Fe^{3+} acceptors have already disappeared after our lowest irradiation dose, and also cannot be detected under optical pumping.

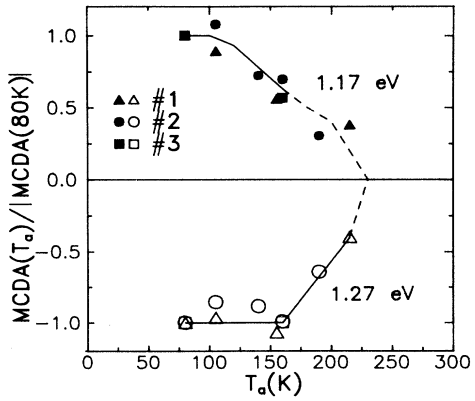

FIG. 4. Annealing of the positive peak at 1.17 eV and the negative peak at 1.27 eV. At 230 K the two bands can no longer be observed.

In contrast to that the MCDA band continues to grow linearly with dose, and reaches an amplitude that is an order of magnitude higher than that of the Fe^{3+} acceptors (Fig. 8). Hence we are left with intrinsic defects whose annealing correlates well with the annealing of the close Frenkel pairs identified by Huang diffuse scattering (HDS),[1] and therefore we attribute these peaks to such pairs and call them FP1 (the largest peak at 1.27 eV) and FP2 (the 1.17-eV peak). A further discrimination in terms of the sublattices or the additional involvement of antisite defects seems too speculative at present; however, attribution of the spectra to isolated vacancies seems unlikely, as these vacancies are stable at least up to RT as discussed below and therefore at least a part of the signal should survive; similarly isolated interstitial atoms seem very unlikely as (although in contrast to some theoretical expectations) no energy level has been observed so far within the band gap of InP or GaAs that could be attributed to interstitial atoms.

B. The 1.06-eV MCDA Band

The spectra observed after annealing at 230 K are dominated by the MCD of the P_{In} antisite that is characterized by the tail of the peak close to the band edge (Fig. 2), and this spectrum does not change much after annealing up to 320 K. However, additional measurements under simultaneous optical excitation through a band-pass filter (BP 1200, transparent region 1160–1270 nm or 0.99–109 eV) show some changes (Fig. 2). The difference between these spectra $MCDA_p$ is plotted in Fig. 5, and shows the characteristic shape of the 1.06-eV band. This band seems to reach its maximum amplitude after annealing at 230–320 K. As shown in Fig. 6 the amplitude of this MCDA seems to be independent of the irradiation dose. This saturation is in agreement with the attribution of this band to an irradiation defect-impurity complex as discussed in Sec. II.

Figure 7 summarizes the buildup and decay of this signal as a function of the annealing temperature. This sig-

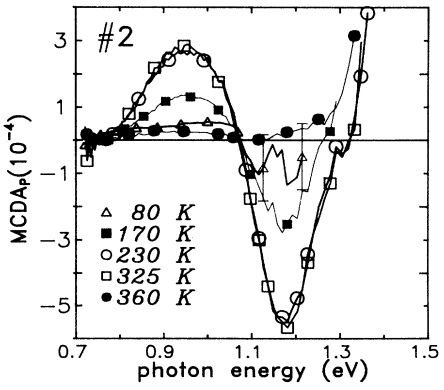

FIG. 5. $MCDA_p$ spectra observed with sample 2 using a bandpass filter BP1200 for the pumping light source. The signal shows a zero crossing point at 1.06 eV and represents the well-known 1.06-eV MCDA band.

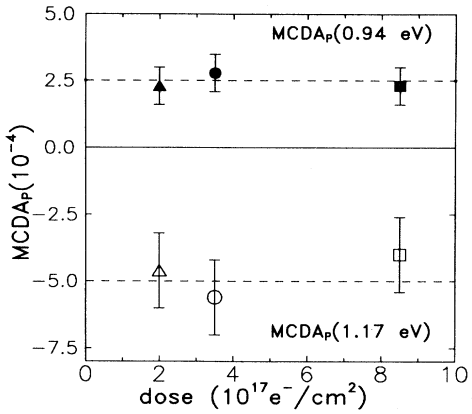

FIG. 6. Dose dependence of the amplitude of the 1.06-eV MCDA band as obtained from the peak heights at 0.94 and 1.17 eV. All measurements were performed after annealing at 325 K.

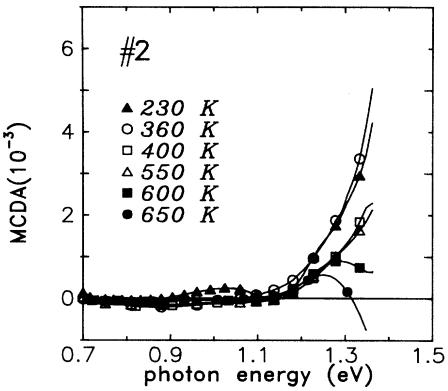

FIG. 8. MCDA spectra observed after annealing between 230 and 650 K for sample 2 ($\phi t = 4\times10^{17}\ e^-/cm^2$). The spectrum observed after annealing at 650 K corresponds to the Fe acceptor that has been observed before irradiation with a similar amplitude.

nal shows a sharp annealing stage between 330 and 360 K, i.e., a complete annealing at the beginning of annealing stage II. There seems to be an indication of the presence of the signal directly after irradiation for sample 1, i.e., the sample with the lowest background due to other defects. This observation indicates that this complex is produced directly during irradiation. However, the signal increases with the annealing of the FP1 and FP2 signals. As the effect of the optical pumping may depend very sensitively on the competition of electron or hole traps and other defect interactions we will make no quantitative conclusions, e.g., a change of the defect concentration or a simple change of the visibility.

C. The P_{In} antisite

After annealing at 230 K the dominating contribution to the MCDA shows characteristic features of the spectrum of the P_{In} antisite (Fig. 2), and Fig. 8 shows changes of the spectra during further annealing. Due to the high absorption close to the band edge only the tail of the characteristic peak of the P_{In} antisite can, however, be resolved. In order to compare the increase of the amplitude, a value at 1.32 eV has been selected and is plotted as a function of the irradiation dose in Fig. 9. Within the errors we observe a linear increase of the signal after annealing at 230 K, as well as after annealing between 450 and 500 K where the high-dose irradiation can be included. Hence there is no saturation of the number of radiation-induced defects.

The annealing of the amplitude at 1.32 eV is summarized in Fig. 10. There is a first decrease by about 50% between 350 and 400 K (the end of stage II) and a final annealing between 550 and 650 K. Figure 8 shows in addition that after the final annealing the MCDA is dominated again by the signal of the Fe acceptor that has the same amplitude as before irradiation.

The attribution of the observed MCDA band to the P_{In} antisite is obvious from the similarity of the generally

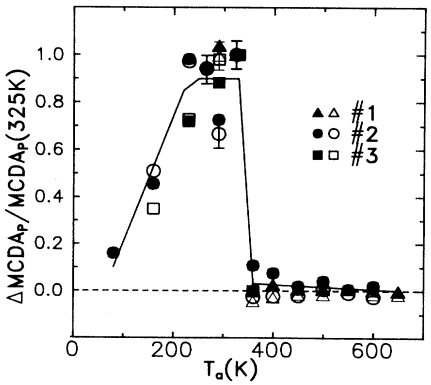

FIG. 7. Growth and annealing behavior of the 1.06-eV MCDA band. The amplitude of the peak at 1.17 eV is shown by the open symbols (similar to Fig. 6), and the peak at 0.94 eV by closed symbols.

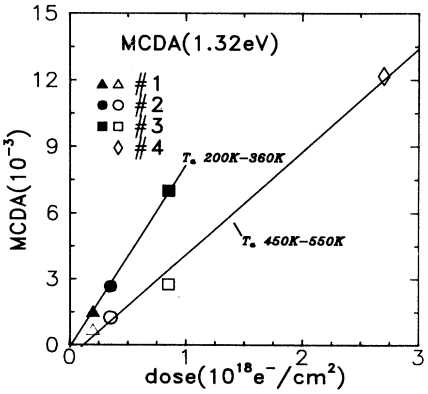

FIG. 9. Amplitude of the MCDA at 1.32 eV, as observed between 200 and 360 K and between 450 and 550 K. The high dose sample 4 could be included for higher temperatures only, as this sample had been warmed to about 80 °C during the additional polishing.

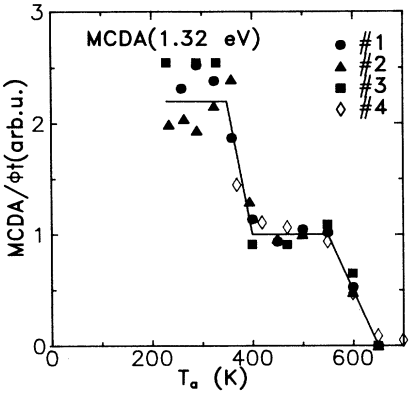

FIG. 10. Annealing of the MCDA amplitude at 1.32 eV that is attributed to P_{In} antisite defects. Data are shown on a normalized scale.

very specific features of the spectra. However, due to the limited range of the spectra some additional comments might be helpful: Similar to the discussion in Sec. III A we observe a linear dose dependence that directly indicates an intrinsic defect; in addition, the annealing behavior of the spectrum excludes an attribution to the complexes[22] of the most abundant Fe doping atoms. The only intrinsic defect observed so far that yields a compatible MCDA spectrum is the P_{In} antisite. The presence of the P_{In}^{+} charge state of the antisite is completely compatible with the expectation (Sec. II A), i.e., a limiting position of E_F at $E_c-(0.3-0.4)$ eV and the location of the $P_{In}^{+/2+}$ level at $E_c-(0.3-0.4)$ eV for bulk samples.[7] The insensitivity of our signal to optical pumping indicates more specifically that for our condition the exact location of these levels is such that nearly all antisites are in the P_{In}^{+} charge state.

D. Optical absorption

The optical-absorption spectra observed after irradiation and annealing up to 650 K are shown for the example of sample 2 in Figs. 11(a) and 11(b). The annealing behavior reveals that these spectra may be considered as a superposition of the 0.77-eV band[15] discussed above and a background that strongly increases close to the band edge. This background might quite generally be understood as a superposition of ionization transitions from many different defects. Figure 12 summarizes the annealing at two characteristic energies of the spectrum, i.e., at 1.07 eV, where the band is dominating, and at 1.34 eV where all other ionization transitions dominate. Figure 12(a) shows a steady increase of the absorption with irradiation dose and a clear annealing stage between 330 and 400 K, that is in full agreement with previous results[15] for the 0.77-eV band. Figure 12(b) shows the band-edge absorption for all samples on a normalized scale. Although we have to consider errors of ≈20% due to the high absorption for the lowest annealing temperatures, we observe a steady annealing starting from the lowest temperature and a decrease by about 60% within stage I. This

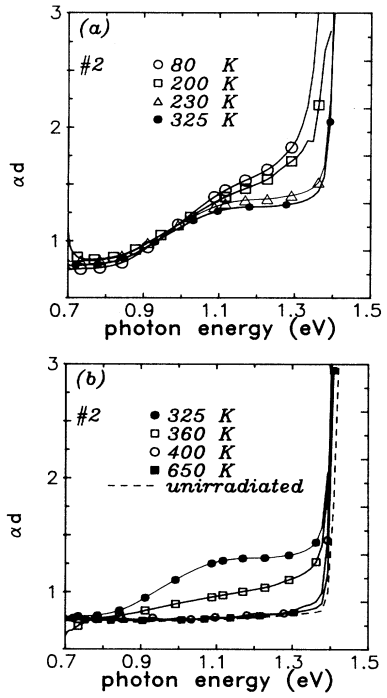

FIG. 11. Optical absorption after irradiation and annealing of sample 2 ($\phi t=3.5\times10^{17}$ e^-/cm^2). (a) Annealing between 80 and 325 K. (b) Annealing between 325 and 650 K.

decrease correlates quite well with the x-ray results,[1] and again indicates a dominating annealing stage I for the intrinsic defects.

IV. DISCUSSION OF THE DEFECT REACTIONS

In this section we will discuss results for the defects and their reactions as they are observed in annealing stages I and II,[23] and in the final annealing stage between 450 and 650 K that we call stage III.

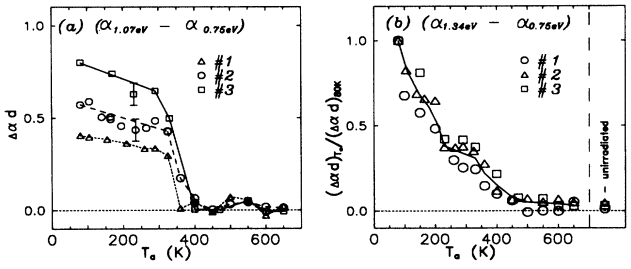

FIG. 12. (a) Annealing of the absorption at 1.07 eV and (b) close to the band edge at 1.34 eV. In order to eliminate the effects of small changes of the reflectivity of the samples after remounting, the value of αd at 0.75 eV that is nearly not affected by the irradiation defects (see Fig. 11) has been subtracted. (a) is given on an absolute scale in order to show the dose dependence (sample 1: 2.0×10^{17}; sample 2: 3.5×10^{17}; sample 3: 8.5×10^{17} e^-/cm^2), and (b) has a normalized scale in order to show the similarity of the annealing after different irradiation doses.

A. Defects and their reactions in stage I ($T_a \leq 250$ K)

Immediately after irradiation we observe a new MCDA spectrum. From the linear increase of the amplitudes with the irradiation dose and from the details of the annealing kinetics up to the final annealing at 230 K we concluded that this spectrum is a superposition of the spectra of two different intrinsic defects FP1 (the 1.27-eV peak) and FP2 (the 1.17-eV peak). As there is no other spectroscopic evidences of intrinsic defects we attribute these peaks to the close FP's that have been shown by HDS to anneal within this temperature range.[1] As long as there is no additional information, e.g., from EPR or ENDOR, further interpretations of these signals seem speculative. The annealing of major intrinsic defects within this temperature range is, however, supported by the annealing of the near-band-edge absorption [see Fig. 12(b)] and by the annealing of vacancy-type defects as shown by position annihilation spectroscopy (PAS) for n-type InP.[24]

Along with the annealing of these FP's we observe the evolution of two MCD spectra that are well known from RT irradiation, i.e., the 1.06-eV band and the P_{In} spectrum. Whereas there is some indication that the 1.06-eV MCDA band is directly formed during irradiation, P_{In} seems to be created by defect reactions. However, the invisibility of the MCDA spectrum of P_{In} at low annealing temperatures might also be due to an irradiation-induced shift of the Fermi level and the corresponding change of the charge state of the defect, e.g., the Fermi level is close to midgap as long as FP1 and FP2 are present, and moves along with the annealing up to the position that is usually observed at RT after high-dose irradiation.[12,16,17] Attempts to make these antisites visible by optical pumping failed, but this failure does not exclude the presence of P_{In} as optical pumping experiments are conclusive only if they are successful. Hence we cannot decide at present whether P_{In} is produced directly during irradiation (e.g., by replacement collisions) or by defect reactions during stage-I annealing. This situation seems very similar to the observations of the As_{Ga}-X_1 complex that is generally only observed after RT annealing of irradiated GaAs,[11,23] i.e., after annealing of close FP's that are basically attributed to the Ga sublattice. This defect has therefore been considered as a reaction product, but we have recently shown that As_{Ga}-X_1 can be directly produced at 4 K.[20]

The linear increase of the P_{In} signal with the irradiation dose seems to be at variance with a tendency toward saturation observed by Deiri *et al.*;[10] instead of a possible difference between 4-K and RT irradiations we suppose, as already discussed by the authors,[10] that their observation of a fast initial increase of the concentration might be due to the shift of the Fermi level of their p-type InP and the consequent visibility of preexisting antisites. Hence our signals correspond to their final smaller slope.

In addition to the MCDA spectra the 0.77-eV band of the optical absorption reveals another intrinsic defect that must have been directly produced during irradiation. In addition, it is remarkable that the magnitude of the 0.77-eV band is not affected by the defect reactions below RT. Consistent with this observation, at low temperatures we obtain an introduction rate of $\Sigma \approx 1$ cm^{-1}, similar to what Brailovskii, Eritsyan, and Grigoryan[15] obtained after RT irradiations (if we use the same calibration of the defect density that was based on the assumption of an oscillator strength of $f \approx 1$). This introduction rate yields defect densities up to 10^{18} cm^{-3}, and indicates again that only intrinsic defects can be involved.

B. Defects and reactions with stage II (330–420 K)

The 1.06-eV MCDA band has been introduced with a concentration that was independent of the irradiation dose, and has therefore been attributed to a defect-impurity complex. This band anneals within a sharp step between 330 and 360 K. These observations are in agreement with the results of RT irradiation of differently doped InP.[13] From the close similarities of the annealing kinetics of this band with the dominant DLTS levels $H4$ and $E11$ (that might also be related to the same defect[26]), it was concluded that these signals correspond to the same defect,[13] probably an impurity complex involving Zn impurities and possibly P interstitials P_i or phosphorus vacancies V_P.[13] If this correlation to $H4$ is correct, the buildup of the MCDA signal (Fig. 7) could reflect the true defect concentration, as similar effects have been reported for $H4$, i.e., direct production during irradiation and an increase of the concentration during stage-I annealing.[23]

Within the temperature range from 330 to 350 K the 0.77-eV band of the optical absorption disappears completely, and indicates the annealing of a major intrinsic defect. There is at present no interpretation of this band; however, there seems to be an obvious correlation to an EPR signal that has been attributed to V_P.[27] This defect has been introduced at RT with a similar introduction rate of ≈ 1 cm^{-1}, and also anneals in a similar way to the 0.77-eV band. As positron annihilation spectroscopy reports vacancy clustering only at higher temperatures,[17,28] this annealing stage might be attributed to the detrapping of P_i and its consequent recombination with V_P.

Finally, within this temperature range we observe a 50% reduction of the P_{In} antisite MCDA signal. This observation might be considered as evidence of the rearrangement of complexes (e.g., by detrapping or trapping of additional P_i) that transform the defect complexes into charge states that are invisible by the MCDA. The alternative possibility of an elimination of the antisite defect itself could be performed by a kick-out mechanism of the mobile In interstitial In_i, or by an exchange mechanism via vacancy migration. The first process seems very unlikely as, if this process would be effective, it should already be effective at lower temperatures; the second process seems unlikely too, as there is no other indication of vacancy migration at that temperature.

C. Final annealing within stage III (420–650 K)

The only signals left above 420 K are a small part of the near-band-edge absorption, that anneals steadily up to 650 K, and the P_{In} MCDA signal. This MCDA is constant up to 550 K, and has completely annealed at 650 K,

where the original signal of the Fe acceptor also indicates a complete annealing. Supported by evidence of vacancy mobility in this temperature range due to PAS,[17,28] this annealing can be explained in a straightforward manner by vacancy migration. These mobile vacancies finally rearrange and anneal the remaining point defect complexes.

V. SUMMARY AND CONCLUSIONS

After low-temperature electron irradiation of InP we observed two resulting MCD spectra, FP1 and FP2, that are attributed to different close Frenkel pairs and that anneal within stage I. This seems to be the first spectroscopic evidence of intrinsic point defects that anneal at low temperatures in InP.

In addition to these signals the known optical fingerprints of several intrinsic defects and of an impurity-defect complex have been investigated over a wide range of defect concentrations and annealing temperatures. The characteristic annealing reactions are schematically summarized in Fig. 13, and compared to the annealing of the Huang diffuse scattering (HDS) intensity that yields an average signal over all defects present in the sample, and which was discussed in Ref. 1. Although the HDS data were taken from the lower irradiation doses, these doses of $\approx 10^{19}$ e^-/cm^2 are still much higher than those of the optical data with doses of $\approx 10^{18}$ e^-/cm^2. Nevertheless, as the x-ray results were linear in dose for $0.8-4.0\times 10^{19}$ e^-/cm^2 and the intrinsic optical defects in the range from 0.02 to 0.3×10^{19} e^-/cm^2, the extrapolation to an overlap of the doses seems meaningful.

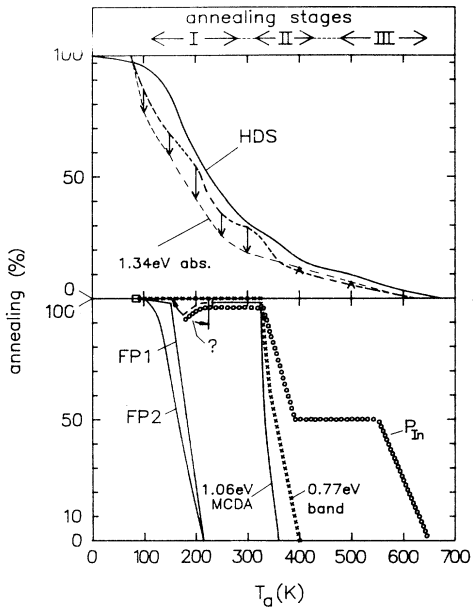

FIG. 13. Comparison of the annealing behavior of InP as observed by different experiments. (a) HDS intensity for the lower irradiation doses of Ref. 1 ($\phi t = 0.8-1.7\times 10^{19}$ e^-/cm^2) and of the near-band-edge absorption at 1.34 eV from Fig. 12(b) ($\phi t = 0.02-0.085\times 10^{19}$ e^-/cm^2). The arrows show the values obtained after subtraction of the contribution of the 0.77-eV band. (b) Annealing of the different fingerprints: FP1, FP2, the 1.06 MCDA band, the 0.77-eV band, and the P_{In} MCDA signal. The question mark indicates that it cannot be decided from the present experiments whether the 1.06-eV MCDA band and the P_{In} signal are invisible below 230 K due to a shift of the Fermi level, or whether the majority of these defects are not yet formed.

In Fig. 13(a) the near-band-edge absorption [at 1.34 eV from Fig. 12(b)] is compared to the annealing of the HDS intensity, and we observe a very similar annealing behavior. The similarity of the annealing curves is not much affected if we eliminate the contribution of 0.77-eV and with its step around 350 K [Fig. 12(a)]. The values obtained by subtraction of this contribution and renormalization are indicated by the arrows given in Fig. 13(a). Hence the conclusion drawn from the HDS about a rather continuous annealing background below the sharp annealing stages observed by spectroscopic methods is supported by the near-band-edge absorption, that yields an average over many different ionization transitions. In addition, we recall the similarity to the annealing reactions in GaAs.[1]

Figure 13(b) shows the annealing of the spectroscopic fingerprints. Within stage I we see the annealing of the Frenkel pairs, and within stage II the annealing of an intrinsic defect (the 0.77-eV absorption band) and that of a defect-impurity complex (the 1.06-eV MCDA band). In addition, the signal of the P_{In} antisites decrease to about 50%. These sharp steps are observed well within stage II, originally defined by DLTS measurements.[23] The final annealing stage is characterized by the disappearing of P_{In}, that can be explained by vacancy migration. It seems remarkable that many of these fingerprints seem to be unaffected by other defect reactions below their final annealing temperature; the only exception is P_{In}, that anneals within two sharp steps (and possibly the growth of the 1.06-eV band and of the P_{In} MCDA in stage I). This behavior would be expected if there is only close pair recombination and no escape of mobile interstitials. However, Fig. 13(a) also shows considerable annealing after the end of the close pair annealing, e.g., between 250 and 330 K, indicating additional defect reactions. The missing interaction of these mobile defects with stage-II defects (the 1.06-eV MCDA band, the 0.77-eV band, and P_{In}) can be understood if all stage-II defects have a charge state that repels the defects that are mobile below 330 K; i.e., at least the dominant type of interstitial atom.

The same repulsion also must be effective during irradiation, if we assume that there is an athermal radiation-induced migration of interstitial atoms in InP. This mobility has been deduced from the formation of impurity-defect complexes during low-temperature irradiation,[29] and there is similar evidence here from the observation of the 1.06-eV MCDA band. From the observed acceleration of the defect annealing by minority-carrier injection, there is additional evidence of such recombination-enhanced defect reactions (REDR's).[29,30] Hence if an impurity is a suitable trap for the interstitial atoms, most of these traps would already be occupied after low irradiation doses, and further defects would be repelled; the alternative, in which the impurities act as nucleation

centers for larger agglomerates, can be excluded, as such agglomerates would be detected by HDS.[1] We must therefore expect that after long-time irradiation most of the mobile interstitial atoms cannot find an extrinsic trap and are retrapped at vacancies and vacancy-antisite complexes that might arise from replacement collisions and are continuously produced. In this way more stable FP complexes are built up. HDS can demonstrate that these complexes also stop growing at a very small size. Hence there are extrinsic as well as intrinsic complexes that repel the most mobile defects during irradiation as well as during low-temperature annealing. The only indication of the evolution of the agglomerates is the shift of stage I to higher temperatures that was observed by the HDS at the highest dose. This shift indicates that on the average more stable agglomerates survive. Again the defect pattern seems to be very similar to that observed with high-dose-irradiated GaAs.

ACKNOWLEDGMENTS

The authors would like to thank Professor W. Schilling for his continuous support of this work and for many stimulating discussions. They are very grateful to Dr. Dworschak and the operating team of the Van de Graaff and to W. Bergs for technical assistance.

[1]K. Karsten and P. Ehrhart, Phys. Rev. B **51**, 10 508 (1995).
[2]I. R. Agool, M. Deiri, and B. C. Cavenett, Semicond. Sci. Technol. **4**, 48 (1989).
[3]A. Göger and J.-M. Spaeth, Semicond. Sci. Technol. **6**, 800 (1991).
[4]M. Rac and J.-M. Spaeth, Solid State Commun. **86**, 213 (1993).
[5]T. A. Kennedy and N. D. Wilsey, Appl. Phys. Lett. **44**, 1089 (1984).
[6]W. M. Chen, P. Dreszer, R. Leon, E. R. Weber, E. Sörman, B. Monemar, B. W. Liang, and C. W. Tu, Mater. Sci. Forum **143-147**, 211 (1994).
[7]H. J. Sun, H. P. Gislason, C. F. Rong, and G. D. Watkins, Phys. Rev. B **48**, 17 092 (1993).
[8]M. Deiri, A. Kana-ah, B. C. Cavenett, T. A. Kennedy, and N. D. Wilsey, J. Phys. C **17**, L793 (1984).
[9]D. Y. Jeon, H. P. Gislason, J. F. Donegan, and G. D. Watkins, Phys. Rev. B **36**, 1324 (1987).
[10]M. Deiri, A. Kana-ah, B. C. Cavenett, T. A. Kennedy, and N. D. Wilsey, Semicond. Sci. Technol. **3**, 706 (1988).
[11]H. P. Gislason, H. Sun, R. E. Peale, and G. D. Watkins, Mater. Sci. Forum **83/87**, 905 (1992).
[12]K. Ando, A. Katsui, D. Y. Jeon, G. D. Watkins, and H. P. Gislason, Mater. Sci. Forum **38/41**, 761 (1989).
[13]H. P. Gislason, D. Jeon, K. Ando, and G. D. Watkins, Mater. Sci. Forum **38/41**, 1145 (1989).
[14]J.-M. Spaeth, M. Fockele, and K. Krambrock, Mater. Sci. Eng. B **13**, 261 (1992).
[15]E. Y. Brailovskii, G. N. Eritsyan, and N. E. Grigoryan, Phys. Status Solidi A **78**, K113 (1993).
[16]E. Y. Brailovskii, F. K. Karapetyan, I. G. Megala, and V. P. Tartachnik, Phys. Status Solidi A **71**, 563 (1982).
[17]V. N. Brudnyi, S. A. Vorobiev, and A. A. Tsoi, Appl. Phys. Lett. A **29**, 219 (1982).
[18]P. J. Stephens, in *Advances in Chemical Physics,* edited by I. Prigogine and S. A. Rice (Wiley, New York, 1976), Vol. 35, p. 197.
[19]A. Pillukat, Report Forschungszentrum Jülich Jül-3005 (1995). ISSN 0366-0885.
[20]H. Hausmann, Report Forschungszentrum Jülich Jül-3005 (1994). ISSN 0944-2952.
[21]A. Goltzené, B. Meyer, and C. Schwab, Mater. Sci. Eng. B **20**, 117 (1993).
[22]E. Y. Brailovskii, I. G. Megela, N. H. Pampuchchyan, and V. V. Teslenko, Phys. Status Solidi A **72**, K109 (1982).
[23]A. Sibille, J. Suski, and M. Gilleron, J. Appl. Phys. **60**, 595 (1986).
[24]M. Törnqvist, J. Nissilä, F. Kiessling, C. Corbel, K. Saarinen, A. P. Seitsonen, and P. Hautojärvi, Mater. Sci. Forum **143/147**, 347 (1994).
[25]A. Pillukat and P. Ehrhart, Mater. Sci. Forum **83/87**, 947 (1992).
[26]T. Bretagnon, G. Bastide, and M. Rouzeyre, Phys. Rev. B **41**, 1028 (1990).
[27]H. J. v. Bardeleben, Solid State Commun. **57**, 137 (1986).
[28]P. J. Schultz, P. J. Simpson, U. G. Akano, and I. V. Mitchell, in *Materials Modification by Energetic Atoms and Ions,* edited by K. S. Grabowski, S. A. Barnett, S. M. Rossnagel, and K. Wasa, MRS Symposia Proceedings No. 268 (Materials Research Society, Pittsburgh, 1992), p. 319
[29]A. Sibille, Phys. Rev. B **35**, 3929 (1987).
[30]K. Ando and A. Katsui, in *Physics of Semiconductors,* edited by E. M. Anastessakis and I. D. Joannopoulos (World Scientific, Singapore, 1990), p. 698.